

Optical coupling at a distance between detuned spherical cavities

Andrey V. Kanaev^{a)}

Center for Optoelectronics and Optical Communications, University of North Carolina at Charlotte,
Charlotte, North Carolina 28223

Vasily N. Astratov^{b)}

Department of Physics and Optical Science, Center for Optoelectronics and Optical Communications,
University of North Carolina at Charlotte, Charlotte, North Carolina 28223

Wei Cai

Department of Mathematics, Center for Optoelectronics and Optical Communications,
University of North Carolina at Charlotte, Charlotte, North Carolina 28223

(Received 16 November 2005; accepted 30 January 2006; published online 15 March 2006)

Using numerical modeling, we observe surprisingly high coupling efficiencies (up to 0.1) between spatially separated spherical cavities with strongly detuned whispering gallery modes. We show that the coupling arises from resonance between a discrete energy eigenstate in the sphere containing the source of light and a continuum of “quasi”-whispering gallery modes with noncircular shape and reduced quality factors in the sphere receiving the electromagnetic energy. Such coupling effects may make possible broad spectral transmission effects in coupled resonator optical waveguides, previously thought to be excluded in a real system with significant size disorder. © 2006 American Institute of Physics. [DOI: 10.1063/1.2186075]

Photonic integrated circuits formed by high quality (Q) cavities can operate as coupled resonator optical waveguides¹ (CROWs) with applications in delay lines,² optical filters,³ and sensor devices. The building blocks of CROW structures can be formed by coupled defects^{4,5} in photonic crystals as well as by resonators with cylindrical⁶ and spherical⁷⁻¹³ symmetry supporting whispering gallery mode (WGM) resonances. Compared to other CROW structures, the circuits of microspheres have several properties that make them uniquely suitable for developing photonic integrated technology. These include the ultimate Q factors¹⁴ of their WGM's ($>10^4$ for 4 μm spheres and up to $\sim 10^9$ for submillimeter spheres) and possibilities to sort cavities according to their resonances¹² and to control their spatial layout⁹ and separations by a variety of micromanipulation techniques.

Strong coupling between two *identical* microspheres with resonant WGM's was studied both experimentally^{15,16} and theoretically.^{17,18} However, in real physical systems of ultrahigh- Q resonators the exact resonant conditions for WGM eigenstates are improbable because of the inevitable size variations of the cavities. It may appear that coupling between detuned cavities is not likely to be efficient since both spatial and spectral overlaps¹⁹ of eigenstates in adjacent spheres may be expected to be diminished in such circuits. For chains of touching polystyrene microspheres with size disorders an attenuation of ~ 3 dB per sphere has been observed⁹ experimentally. Developing applications of such structures requires knowledge of basic mechanisms of optical coupling between cavities as a function of their detuning and intercavity gap sizes. For applications in slow light structures a particularly interesting case is represented by the regime of weak coupling between separated cavities.

In this letter using techniques of numerical modeling we show that the coupling between spatially separated detuned cavities can be surprisingly strong (up to 10%). We show that the interaction arises due to coupling between whispering gallery modes in one sphere and a previously overlooked continuum of states in the other sphere. The coupling mechanism resembles the well-known Fano resonances²⁰ between a continuum and a discrete level. The continuum of states is formed by quasi-WGMs with noncircular shape and reduced Q factors induced in the adjacent sphere. This mechanism may play an important role in efficient optical transport phenomena in multiple cavity systems.

The central idea of our numerical studies of coupling phenomena is based on using one of the spheres as a source (S) of light and calculating the spectra of electromagnetic (EM) energy deposited in a second sphere considered as a passive receiver (R) of radiation. To provide maximal use of the interresonator gap region as a “coupler” between individual cavities we excited modes of the bisphere system in the xz plane containing axis of bisphere (x), see Figs. 1(a) and 1(b). The modeling was performed using three-dimensional (3D) finite difference time domain *FullWAVE*TM software.²¹ The discretization grid parameter was equal to $1/16$ of the center pulse wavelength $\lambda = 550$ nm in each dimension. We used a 3.3 fs transverse electric (TE) polarized built-in source of light to generate a comb of WGM resonances with various radial (n), angular (l), and azimuthal (m) mode numbers.²² The source wave front was generated on the half a wavelength square plane inside the S sphere placed perpendicular to its surface at $\lambda/16$ depth with the direction of emission at 45° to the x axis as indicated in Figs. 1(a) and 1(b). To calculate the spectra of the EM energy deposited in the R sphere we used a Fourier transform of the electrical field spatially averaged over several points on the surface of the R sphere in the xz plane.

We begin our studies by calculating the spectra of eigenstates in 3 and 2.4 μm dielectric ($n=1.59$) cavities obtained by modeling energy spectra in the R sphere with the same

^{a)}Present address: SFA Inc., 2200 Defense Highway, Crofton, MD 21114.

^{b)}Author to whom correspondence should be addressed; electronic mail: astratov@uncc.edu

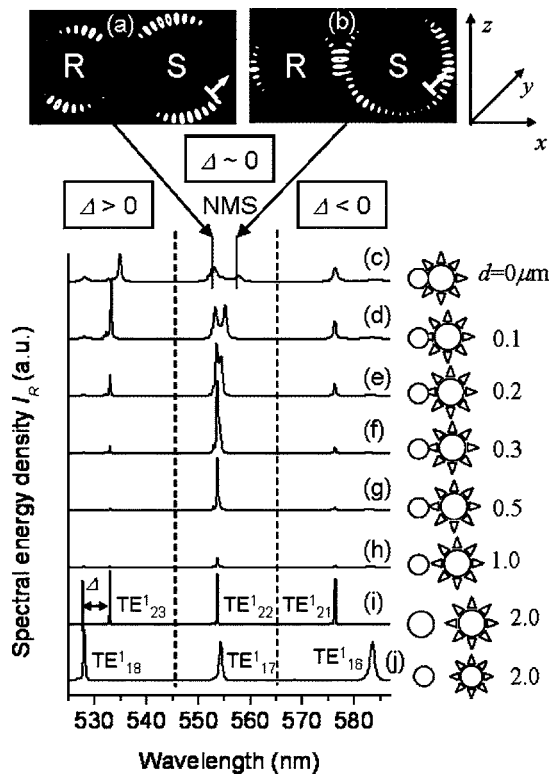


FIG. 1. (a) Antibonding photonic molecular state in the xz plane calculated for touching a $3 \mu\text{m}$ sphere (S) containing source of light and a $2.4 \mu\text{m}$ receiving sphere (R) at 552.9 nm, (b) bonding state at 557.9 nm. The NMS is indicated. Spectral energy densities deposited in the R sphere for different distances d between microresonators: (c) touching case (top), (d) $0.1 \mu\text{m}$, (e) $0.2 \mu\text{m}$, (f) $0.3 \mu\text{m}$, (g) $0.5 \mu\text{m}$, (h) $1.0 \mu\text{m}$, (i) $2 \mu\text{m}$, and (j) $2 \mu\text{m}$. The sizes of bispheres under study: (c)–(h) $3/2.4 \mu\text{m}$, (i) $3/3 \mu\text{m}$, and (j) $2.4/2.4 \mu\text{m}$. The spectra (i) and (j) are magnified for clarity. Three cases with different detuning (Δ) between the closest eigenstates in S and R cavities are separated by vertical dashed lines.

size as the S sphere. In these calculations the cavities were separated by $d=2 \mu\text{m}$ resulting in extremely weak coupling. As illustrated in Fig. 1(i) for a $3/3 \mu\text{m}$ bisphere such a spectrum illustrates a series of peaks with $Q \sim 2 \times 10^3$ and 21 nm separations around $\lambda=530$ nm consistent with the series of fundamental TE_l^m WGM eigenstates with $n=1$ and $l=m=21, 22, 23$ in a $3 \mu\text{m}$ sphere. For a $2.4/2.4 \mu\text{m}$ bisphere the corresponding spectrum displays broader peaks ($Q \sim 10^3$) with larger separations (26 nm) as seen in Fig. 1(j).

The focus of our studies was on coupling effects in a system formed by markedly different spheres with 3 and $2.4 \mu\text{m}$ diameters. Due to the fact that each resonator possesses its own comb of WGM frequencies, we were able to study coupling phenomena for a number of situations with different detuning (Δ) between closest resonances as well as for different separations (d) between the S ($3 \mu\text{m}$) and R ($2.4 \mu\text{m}$) cavities, as illustrated in Figs. 1(c)–1(h). Three WGM eigenstates ($\text{TE}_{23}^1 - \text{TE}_{21}^1$) dominate in the spectrum of the S sphere in this range as seen in Fig. 1(i). Because coupling is provided in the vicinity of closest eigenstates in the S and R cavities, we can distinguish three cases in Fig. 1: (1) is the nearly resonant case with $\Delta = \lambda(\text{TE}_{22}^1) - \lambda(\text{TE}_{17}^1) = -0.5$ nm, (2) corresponds to $\Delta = \lambda(\text{TE}_{23}^1) - \lambda(\text{TE}_{18}^1) = 5$ nm, and (3) corresponds to $\Delta = \lambda(\text{TE}_{21}^1) - \lambda(\text{TE}_{16}^1) = -7.5$ nm.

We start the analysis from the touching sphere position ($d=0$) where the regime of strong coupling is evident in the near resonant case (1) demonstrating marked normal mode

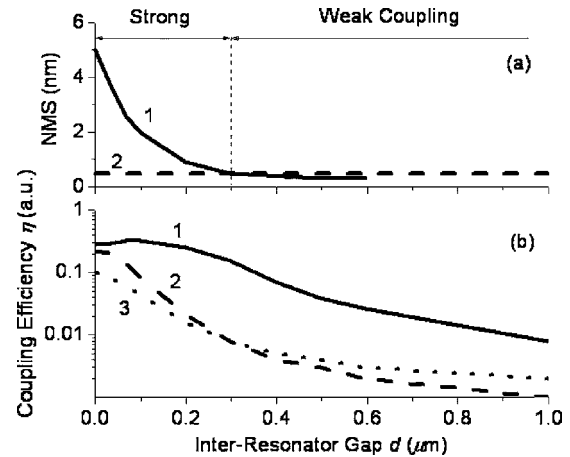


FIG. 2. (a) NMS in nearly resonant case, $\Delta = \lambda(\text{TE}_{22}^1) - \lambda(\text{TE}_{17}^1) = -0.5$ nm, as a function of the inter-sphere gap sizes d (solid line 1). The dashed line 2 indicates the linewidth (0.5 nm) of the TE_{17}^1 resonance. (b) The coupling efficiency (η) is represented as a function of distance d . The solid line 1 represents the nearly resonant case with $\Delta = -0.5$ nm, the dashed line 2 corresponds to $\Delta = 5$ nm, and the dotted line 3 corresponds to $\Delta = -7.5$ nm. The coupling efficiency was calculated as: $\eta = E_R/E_S$, where the total energy $E_{R(S)}$ deposited in the $R(S)$ cavity was estimated by integrating the area under the calculated spectral peaks in the $R(S)$ sphere in each of three cases (1)–(3).

splitting (NMS= 5 nm), see Fig. 1(c). The strong coupling is defined as a regime where NMS exceeds the linewidth of the individual resonances. In contrast in the weak coupling regime the positions of the resonances are not perturbed by their interaction. The strongly coupled nature of the modes at 552.9 and 557.9 nm was verified by propagation of light pulses with bandwidth comparable to the width of the coupled resonances. A classical antibonding molecular state is seen in Fig. 1(a) for the shorter wavelength (552.9 nm) component where the energy is concentrated away from the bisphere axis. For the longer wavelength component (557.9 nm) we observed the corresponding bonding state, Fig. 1(b), where the energy is concentrated at the touching point and along the axis of bisphere. Increasing the separation between the spheres leads to gradual transition to weak coupling as seen in Figs. 1(c)–1(h). In the nearly resonant case (1) the splitting between the coupled resonances is reduced to ~ 0.5 nm for $d=0.3 \mu\text{m}$, as illustrated in Fig. 2(a).

As a measure of the total energy (E_R) deposited in the R cavity in each of three cases (1)–(3) we used the area under coupled spectral peaks: $E_R \sim \int_{\lambda_-}^{\lambda_+} I_R(\lambda) d\lambda$, where $I_R(\lambda)$ is the spectral energy density, $(\lambda_- - \lambda_+)$ is the range of wavelengths spanning both coupled resonances in the R sphere: 550 – 560 nm in case (1), 526 – 536 nm in case (2), and 575 – 585 nm in case (3). A rough estimate of the coupling efficiency (η) was obtained by normalizing E_R by similarly estimated energy in the S sphere: $\eta = E_R/E_S$, where E_S is proportional to the area under the calculated peaks in the S sphere within the same spectral interval. In the weak coupling regime in all three cases (1)–(3) the spectra of the S sphere contain a single resonance with the same spectral position as that in the R sphere. In the strong coupling regime, however, along with the bonding and antibonding states with the same spectral positions in the S and the R spheres the spectra of the S sphere contained additional peaks due to uncoupled modes, which were also included in the estimation of E_S . For this reason the parameter η represents only a

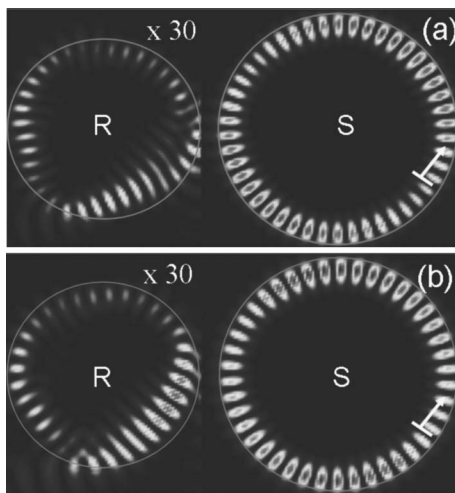


FIG. 3. Mapping of the intensity distribution in the xz bisphere plane at (a) 532.9 nm corresponding to the TE_{23}^1 mode in the S sphere and (b) 576.2 nm corresponding to the TE_{21}^1 mode in the S sphere. The intersphere separation is $0.2 \mu\text{m}$. The intensity in the R sphere is multiplied by 30 to show the distorted noncircular quasi-WGM induced in the R sphere.

low limit of coupling efficiency for strongly coupled modes.

In the nearly resonant case (1) the coupling efficiency exhibits a maximum ($\eta=0.33$) at separations $d\sim 0.1 \mu\text{m}$, see curve 1 in Fig. 2(b). This maximum is indicative of a regime of critical coupling¹⁹ referring to the condition in which coupling loss matches internal resonator loss. At larger separations ($d>0.3 \mu\text{m}$) η decays with $\sim 0.2 \mu\text{m}$ attenuation length. In the detuned cases (2) and (3) the transition to weak coupling occurs at shorter distances $d\sim 0.1 \mu\text{m}$ as indicated by the same positions of the peaks in the spectra of the R sphere and corresponding eigenstates in the S sphere, see the 532.9 and 576.2 nm peaks in Fig. 1(d). The efficiencies of coupling between the detuned cavities are unexpectedly high (up to ~ 0.1) in these cases. An attempt to estimate the energy transfer between two cavities in a weak coupling regime using a coupled mode theory¹⁹ leads to vanishingly small efficiencies due to almost zero spectral overlap of eigenstates in cases (2) and (3).

The nature of the modes excited in bisphere system in such cases was revealed by propagating pulses with the bandwidth comparable to the width of the resonance. Such EM intensity maps in the xz plane calculated for the bisphere with $0.2 \mu\text{m}$ separation for the 532.9 and 576.2 nm peaks is represented in Figs. 3(a) and 3(b) correspondingly. They display the expected undistorted circularly symmetric TE_{23}^1 [Fig. 3(a)] and TE_{21}^1 [Fig. 3(b)] modes in the source S sphere, whereas the modes induced in the R sphere exhibit an irregular noncircular shape. The shape of such quasi-WGM is found to be independent of the location of source of plane waves along the circumference of the S sphere. This mode sets a shorter optical path inside the R cavity required for phase matching with the mode in the S sphere dictating the coupling frequency. The noncircular distortion of such quasi-WGM leads to increased leakage of light from the cavity and to reduced effective Q factors for such modes. It is important to note, however, that the quasi-WGM's have a continuous spectrum because their shape can be continuously adjusted to variations of the frequency. Such coupling between a discrete energy state (true WGM excited in the S cavity) and a continuum of quasi-WGM states in the R cavity resembles Fano resonance²⁰ phenomena observed in spectra of photonic

crystal waveguides²³ and side-coupled waveguide-cavity²⁴ systems. The resonances in the R sphere, however, do not display asymmetric line shapes^{23,24} characteristic of the Fano effect. This is related to the fact that the S -to- R transmission properties in bispheres are vanishingly small outside the resonances that make the interference between a continuum and a discrete level underlying formation of such asymmetric line shapes difficult to observe.

In conclusion, we show that the weak coupling between separated and size-mismatched cavities with strongly detuned eigenstates exhibits surprisingly high efficiencies up to 0.1. The coupling is provided due to excitation of modes with distorted noncircular shape and reduced quality factors. Such modes may play a very important role in the optical transport properties of disordered dielectric resonators with circularly symmetric properties including microdisks, toroids, and spheres.

The authors thank M. S. Skolnick, G. Gbur, M. A. Fiddy, and M. Sumetsky for stimulating discussions. This work was supported by ARO under Grant No. W911NF-05-1-0529 and by NSF under Grants No. CCF-0513179 and No. DMS-0408309 as well as, in part, by funds provided by The University of North Carolina at Charlotte. W.C. acknowledges support from the DOE under Grant No. DEFG0205ER25678. A.V.K. was supported by DARPA Grant No. DAAD 19-03-1-0092.

- ¹A. Yariv, Y. Xu, R. K. Lee, and A. Scherer, *Opt. Lett.* **24**, 711 (1999).
- ²G. Lenz, B. J. Eggleton, C. K. Madsen, and R. E. Slusher, *IEEE J. Quantum Electron.* **37**, 525 (2001).
- ³B. E. Little, S. T. Chu, H. A. Haus, J. Foresi, and J.-P. Laine, *J. Lightwave Technol.* **15**, 998 (1997).
- ⁴S. Oliver, C. Smith, M. Rattier, H. Benisty, C. Weisbuch, T. F. Krauss, R. Houdre, and U. Oesterle, *Opt. Lett.* **26**, 1019 (2001).
- ⁵A. D. Bristow, D. M. Whittaker, V. N. Astratov, M. S. Skolnick, A. Tahraoui, T. F. Krauss, M. Hopkinson, M. P. Croucher, and G. A. Gehring, *Phys. Rev. B* **68**, 033303 (2003).
- ⁶S. Deng, W. Cai, and V. N. Astratov, *Opt. Express* **12**, 6468 (2004).
- ⁷H. Furukawa and K. Tenjimbayashi, *Appl. Phys. Lett.* **80**, 192 (2002).
- ⁸H. Guo, H. Chen, P. Ni, Q. Zhang, B. Cheng, and D. Zhang, *Appl. Phys. Lett.* **82**, 373 (2003).
- ⁹V. N. Astratov, J. P. Franchak, and S. P. Ashili, *Appl. Phys. Lett.* **85**, 5508 (2004).
- ¹⁰B. M. Möller, U. Woggon, M. V. Artemyev, and R. Wannemacher, *Phys. Rev. B* **70**, 115323 (2004).
- ¹¹Y. P. Rakovich, J. F. Donegan, M. Gerlach, A. L. Bradley, T. M. Connolly, J. J. Boland, N. Gaponik, and A. Rogach, *Phys. Rev. A* **70**, 051801(R) (2004).
- ¹²Y. Hara, T. Mukaiyama, K. Takeda, and M. Kuwata-Gonokami, *Phys. Rev. Lett.* **94**, 203905 (2005).
- ¹³B. M. Möller, U. Woggon, and M. V. Artemyev, *Opt. Lett.* **30**, 2116 (2005).
- ¹⁴L. Gorodetsky, A. A. Savchenkov, and V. S. Ilchenko, *Opt. Lett.* **21**, 453 (1996).
- ¹⁵T. Mukaiyama, K. Takeda, H. Miyazaki, Y. Jimba, and M. Kuwata-Gonokami, *Phys. Rev. Lett.* **82**, 4623 (1999).
- ¹⁶Y. Hara, T. Mukaiyama, K. Takeda, and M. Kuwata-Gonokami, *Opt. Lett.* **28**, 2437 (2003).
- ¹⁷K. A. Fuller, *Appl. Opt.* **30**, 4716 (1991).
- ¹⁸H. Miyazaki and Y. Jimba, *Phys. Rev. B* **62**, 7976 (2000).
- ¹⁹H. A. Haus, *Waves and Fields in Optoelectronics* (Prentice Hall, Englewood Cliffs, NJ, 1984).
- ²⁰U. Fano, *Phys. Rev.* **124**, 1866 (1961).
- ²¹FullWave™, Rsoft Design Group Inc., U.R.L.: www.rsoftdesign.com.
- ²²For a review see articles in *Optical Processes in Microcavities*, edited by R. K. Chang and A. J. Campillo (World Scientific, Singapore, 1996).
- ²³V. N. Astratov, D. M. Whittaker, I. S. Culshaw, R. M. Stevenson, M. S. Skolnick, T. F. Krauss, and R. M. De La Rue, *Phys. Rev. B* **60**, R16255 (1999).
- ²⁴S. Fan, *Appl. Phys. Lett.* **80**, 908 (2002).